

SLAC-PUB-6925

July 1995

A STUDY OF RAPIDITY GAPS IN $e^+e^- \rightarrow Z^0$ EVENTS*

The SLD Collaboration**

Stanford Linear Accelerator Center

Stanford University, Stanford, CA 94309

ABSTRACT

Distributions of rapidity gaps between charged particles are studied in Z^0 decay events recorded by the SLD experiment at SLAC. We find that our measured gap spectra are well modelled by standard Monte Carlo simulations of hadronisation. Gaps in hadronic events are studied as a function of event primary flavor, jet multiplicity and total charged multiplicity.

Contributed to the International Europhysics Conference on High Energy Physics (HEP 95), Brussels, Belgium, July 27 - August 2, 1995

*This work was supported by Department of Energy contracts: DE-FG02-91ER40676 (BU), DE-FG03-92ER40701 (CIT), DE-FG03-91ER40618 (UCSB), DE-FG03-92ER40689 (UCSC), DE-FG03-93ER40788 (CSU), DE-FG02-91ER40672 (Colorado), DE-FG02-91ER40677 (Illinois), DE-AC03-76SF00098 (LBL), DE-FG02-92ER40715 (Massachusetts), DE-AC02-76ER03069 (MIT), DE-FG06-85ER40224 (Oregon), DE-AC03-76SF00515 (SLAC), DE-FG05-91ER40627 (Tennessee), DE-AC02-76ER00881 (Wisconsin), DE-FG02-92ER40704 (Yale); National Science Foundation grants: PHY-91-13428 (UCSC), PHY-89-21320 (Columbia), PHY-92-04239 (Cincinnati), PHY-88-17930 (Rutgers), PHY-88-19316 (Vanderbilt), PHY-92-03212 (Washington); the UK Science and Engineering Research Council (Brunel and RAL); the Istituto Nazionale di Fisica Nucleare of Italy (Bologna, Ferrara, Frascati, Pisa, Padova, Perugia); and the Japan-US Cooperative Research Project on High Energy Physics (Nagoya, Tohoku).

1 Introduction

Since the initial observation of hadronic jets, rapidity has been used to characterize the momentum of particles in jets in a frame-invariant manner [1]. Recently Bjorken [2] has called attention to the production of color-singlet systems in hard diffractive hadron-hadron processes which would be characterized by a large gap in the event rapidity spectrum. Rapidity gaps have been observed at Fermilab [3, 4] and DESY [5, 6] although their origin is not yet understood. The interpretation of these phenomena is dependent on an understanding of the spectrum of rapidity gaps arising in the hadronization process, and in particular on a knowledge of the probability of random fluctuations producing large gaps.

Bjorken et al. [7] have discussed e^+e^- annihilation to large rapidity gap events via a color screening mechanism. We present the first measurements of rapidity gap spectra in e^+e^- annihilation. In particular we study the dependence of the measured rapidity gap spectra on the event primary flavor and on the event jet topology.

We describe the detector, the event trigger and the event selection criteria applied to the data in Section 2. In Section 3 we define the observables used in this analysis. The analysis of the data is described in Section 4, and conclusions are presented in Section 5.

2 Apparatus and Hadronic Event Selection

The e^+e^- annihilation events produced at the Z^0 resonance by the SLAC Linear Collider (SLC) have been recorded using the SLC Large Detector (SLD). A general description of the SLD can be found elsewhere [8]. Charged tracks are measured in the central drift chamber (CDC) and in the vertex detector (VXD) [9]. Momentum measurement is provided by a uniform axial magnetic field of 0.6 T. Particle energies are measured in the Liquid Argon Calorimeter (LAC) [10], which contains both electromagnetic and hadronic sections, and in the Warm Iron Calorimeter [11].

Three triggers were used for hadronic events. The first required a total LAC electromagnetic energy greater than 12 GeV; the second required at least two well-separated tracks in the CDC; and the third required at least 4 GeV in the LAC and one track in the CDC. A selection of hadronic events was then made by two independent methods, one based on the topology of energy depositions in the calorimeters, the other on the number and topology of charged tracks measured in the CDC.

The analysis presented here used the charged tracks measured in the CDC and VXD. A set of selection cuts was applied to the data to select well-measured tracks and events well-contained within the detector acceptance. Charged tracks were required to have (i) a closest approach transverse to the beam axis within 5 cm, and within 10 cm along the axis from the measured interaction point; (ii) a polar angle θ with respect to the beam axis within $|\cos\theta| < 0.80$; and (iii) a momentum transverse to the beam axis $p_{\perp} > 0.15$ GeV/c. Events were required to have (i) a minimum of five such tracks; (ii) a thrust axis [12] direction within $|\cos\theta_T| < 0.71$; and (iii) a total visible energy E_{vis} of at least 20 GeV, which was calculated from the selected tracks assigned the charged pion mass. From our 1994-95 data sample we have used 34,890 events which passed these cuts. The efficiency for selecting hadronic events satisfying the $|\cos\theta_T|$ cut was estimated to be above 96%. The background in the selected event sample was estimated to be $0.3 \pm 0.1\%$, dominated by $Z^0 \rightarrow \tau^+\tau^-$ events. Distributions of single particle and event topology observables in the selected events were found to be well described by Monte Carlo models of hadronic Z^0 decays [13, 14] combined with a simulation of the SLD.

3 Definitions of Observables and Event Tags

A Rapidity gaps

Charged particle rapidity is defined by

$$\eta = 0.5 \ln \frac{E + p_{\parallel}}{E - p_{\parallel}}, \quad (1)$$

where E is the particle energy calculated from its measured momentum and a presumed charged pion mass and p_{\parallel} is its momentum component along the thrust axis of the event. We order the N charged particles in an event by their rapidity, which defines $N - 1$ rapidity gaps between pairs of particles taken as nearest neighbors in the rapidity ordering. The largest rapidity gap in the event, $\Delta\eta_{max}$, is defined as the largest of the $N - 1$ gaps between nearest neighbors.

We define the average gap size by

$$\langle \Delta\eta \rangle = \frac{\eta_{max} - \eta_{min}}{N - 1}, \quad (2)$$

where η_{max} is the greatest particle rapidity in the event and η_{min} is the least particle rapidity.

B Flavor tagging

Events were classified as being of light (u, d or s) or heavy (b) flavor based on impact parameters of charged tracks measured in the vertex detector. The 22,908 events containing no track with normalized transverse impact parameter with respect to the interaction point $b/\sigma_b > 3$ were assigned to the light flavor sample. The 4,669 events containing three or more tracks with normalized transverse impact parameter with respect to the interaction point $b/\sigma_b > 3$ were assigned to the heavy flavor sample. The light flavor content of the light sample was estimated from Monte Carlo simulations to be 85% and the b flavor content of the heavy sample was estimated to be 89%. A full discussion of flavor tagging can be found in [15].

C Jet tagging

The JADE jet-finding algorithm [16] was used to define the number of jets in an event. The values 0.005, 0.02 and 0.13 of the scaled invariant mass, y_{cut} , were used. For $y_{cut} = 0.005$ the sample contained 4,280 2-jet and 30,567 ≥ 3 -jet events; for $y_{cut} = 0.02$ 13,314 2-jet and 15,693 ≥ 3 -jet events, and for $y_{cut} = 0.13$ 32,281 2-jet and 2,504 ≥ 3 -jet events.

4 Rapidity Gaps Analysis

The measured distributions of $|\eta|$, $\langle \Delta\eta \rangle$, and $\Delta\eta_{max}$ are shown in Figures 1a, b and c respectively. Also shown are the predictions of the JETSET 7.4 Monte Carlo program [17] for the simulation of Z^0 decays, combined with a simulation of the SLD, and with the same cuts as applied to the data. The simulation models the data well except at the high end of the rapidity gap spectra. This small discrepancy is due to $\tau^+\tau^-$ event contamination of the hadronic sample. Also shown in Figures 1b and c is a KORALZ [18] simulation of $Z^0 \rightarrow \tau^+\tau^-$ combined with a simulation of the SLD and subjected to the same cuts as the data. This simulation describes the high $\langle \Delta\eta \rangle$ and $\Delta\eta_{max}$ regions well.

We have performed a Monte Carlo study to investigate further the observed spectra. In each of Figures 2a, b and c we show the following three samples:

- (1) Generator-level events including all charged and neutral final state particles except neutrinos.
- (2) Generator-level events including only stable charged final-state particles.
- (3) Events with detector simulation, including only charged tracks, and with the track and event selection cuts applied.

The rapidity spectra for cases (1) - (3) are very similar (Fig. 2a), but the gap spectra are noticeably different (Figs. 2b, c). In the step from (1) to (2) the reduction in the number of final-state particles produces a widening of both gap distributions and an increase in the peak positions. Going from (2), generator-level, to (3), detector-level,

narrows the distributions and decreases the peak positions of both gap distributions. This is due to an increase in the number of charged particles from interactions in the detector, particularly from conversion of photons from π^0 decays.

We have investigated the dependence of the measured spectra of the three observables, $|\eta|$, $\langle \Delta\eta \rangle$, and $\Delta\eta_{max}$ on jet topology and event primary flavor. For the jet study we examined the spectra separately for 2-jet and ≥ 3 -jet event samples. The number of jets in an event is defined by the y_{cut} value used in the jet-finding algorithm. A smaller value of y_{cut} corresponds to a smaller invariant mass cutoff in the combining of particles into jets and implies that fewer events will be classified as 2-jet events, and that these events will be more collimated along the thrust axis than 2-jet events defined with a larger value of y_{cut} .

The rapidity spectra for 2-jet and ≥ 3 -jet events for $y_{cut} = 0.005, 0.02, 0.13$ are shown in Figures 3a, b and c. The peak of the 2-jet spectrum moves to lower rapidity as y_{cut} is increased and less collimated events are added to the 2-jet sample. As these events leave the ≥ 3 -jet sample, that spectrum tends to become narrower as it loses its higher rapidity particles. In all cases the Monte Carlo reproduces the data.

The $\langle \Delta\eta \rangle$ and $\Delta\eta_{max}$ gap spectra are shown in Figures 4a, b and c and in Figures 5a, b and c respectively. In each case they are separated into 2-jet and ≥ 3 -jet event samples for the three values of y_{cut} . The peak of the 2-jet spectra moves to lower gap size as y_{cut} is increased and as less collimated events are added to the 2-jet sample. As these events leave the ≥ 3 -jet sample, that spectrum tends to become narrower as it loses its larger gap events. Again, the Monte Carlo reproduces the data.

For the study of the dependence of the measured spectra on event flavor we selected samples of light (u, d and s) quark events and heavy (b) quark events. These spectra are shown in Figures 6a, b, and c. The rapidity spectrum of the b-tagged sample is relatively flat out to rapidity of 2.2 followed by a sharp drop off. The light quark spectrum peaks at a low value of rapidity and falls slowly. This difference can be explained by the kinematics of B-hadron decays. For the gap observables, $\langle \Delta\eta \rangle$ and

$\Delta\eta_{max}$, we observe that the light-quark sample has a bigger tail of events with large gaps but the peaks of the distributions are at about the same place as the heavy quark sample

5 Summary

We have studied the observables, rapidity, event average rapidity gap, and event maximum rapidity gap in $e^+e^- \rightarrow Z^0 \rightarrow q\bar{q}$ events. We have studied the dependence on jet topology and looked separately at light and heavy quark flavor samples. We find that the JETSET 7.4 event generator with detector simulation models the qualitative features of these dependences well, particularly in the large rapidity gap region.

Acknowledgements

We thank the personnel of the SLAC accelerator department and the technical staffs of our collaborating institutions for their efforts which has resulted in the successful operation of the SLC and the SLD.

References

- [1] See eg: M. Althoff *et al.*, Z. Phys. **C22** (1984) 307.
- [2] J. D. Bjorken, Phys. Rev. **D47** (1993) 101.
- [3] F. Abe *et al.*, Phys. Rev. Lett. **74** (1995) 855.
- [4] S. Abachi *et al.*, Phys. Rev. Lett. **72** (1994) 2332.
- [5] T. Ahmed *et al.*, Nuc. Phys. **B429** (1994) 477.
- [6] M. Derrick *et al.*, Phys. Lett. **B332** (1994) 228.

- [7] J. Bjorken *et al.*, Phys. Lett. **B286** (1992) 153.
- [8] SLD Design Report, SLAC Report 273 (1984).
- [9] C. J. S. Damerell *et al.*, Nucl. Inst. Meth. **A288** (1990) 288.
- [10] D. Axen *et al.*, Nucl. Inst. Meth. **A328** (1993) 472.
- [11] A. C. Benvenuti *et al.*, Nucl. Inst. Meth. **A290** (1990) 353.
- [12] S. Brandt *et al.*, Phys. Lett. **12** (1964) 57.
E. Farhi, Phys. Rev. Lett. **39** (1977) 1587.
- [13] T. Sjöstrand and M. Bengtsson, Comp. Phys. Comm. **43** (1987) 367.
- [14] G. Marchesini *et al.*, Comp. Phys. Comm. **67** (1992) 465.
- [15] SLD Collab., K. Abe *et al.*, SLAC-PUB 6569, submitted to Phys. Rev. D.
- [16] JADE Collab., W. Bartel *et al.*, Z. Phys. **C33** (1986) 23.
- [17] T. Sjöstrand, CERN-TH.7112/93 (1993)
- [18] S. Jadach, B.F.L. Ward, Z. Was, Comp. Phys. Comm. **66** (1991) 276.

List of Authors

** K. Abe,⁽²⁹⁾ I. Abt,⁽¹⁴⁾ C.J. Ahn,⁽²⁶⁾ T. Akagi,⁽²⁷⁾ N.J. Allen,⁽⁴⁾ W.W. Ash,^{(27)†}
D. Aston,⁽²⁷⁾ K.G. Baird,⁽²⁴⁾ C. Baltay,⁽³³⁾ H.R. Band,⁽³²⁾ M.B. Barakat,⁽³³⁾
G. Baranko,⁽¹⁰⁾ O. Bardon,⁽¹⁶⁾ T. Barklow,⁽²⁷⁾ A.O. Bazarko,⁽¹¹⁾ R. Ben-David,⁽³³⁾
A.C. Benvenuti,⁽²⁾ T. Bienz,⁽²⁷⁾ G.M. Bilei,⁽²²⁾ D. Bisello,⁽²¹⁾ G. Blaylock,⁽⁷⁾
J.R. Bogart,⁽²⁷⁾ T. Bolton,⁽¹¹⁾ G.R. Bower,⁽²⁷⁾ J.E. Brau,⁽²⁰⁾ M. Breidenbach,⁽²⁷⁾
W.M. Bugg,⁽²⁸⁾ D. Burke,⁽²⁷⁾ T.H. Burnett,⁽³¹⁾ P.N. Burrows,⁽¹⁶⁾ W. Busza,⁽¹⁶⁾
A. Calcaterra,⁽¹³⁾ D.O. Caldwell,⁽⁶⁾ D. Calloway,⁽²⁷⁾ B. Camanzi,⁽¹²⁾ M. Carpinelli,⁽²³⁾
R. Cassell,⁽²⁷⁾ R. Castaldi,^{(23)(a)} A. Castro,⁽²¹⁾ M. Cavalli-Sforza,⁽⁷⁾ E. Church,⁽³¹⁾

H.O. Cohn,⁽²⁸⁾ J.A. Coller,⁽³⁾ V. Cook,⁽³¹⁾ R. Cotton,⁽⁴⁾ R.F. Cowan,⁽¹⁶⁾
 D.G. Coyne,⁽⁷⁾ A. D'Oliveira,⁽⁸⁾ C.J.S. Damerell,⁽²⁵⁾ M. Daoudi,⁽²⁷⁾ R. De Sangro,⁽¹³⁾
 P. De Simone,⁽¹³⁾ R. Dell'Orso,⁽²³⁾ M. Dima,⁽⁹⁾ P.Y.C. Du,⁽²⁸⁾ R. Dubois,⁽²⁷⁾
 B.I. Eisenstein,⁽¹⁴⁾ R. Elia,⁽²⁷⁾ D. Falciai,⁽²²⁾ M.J. Fero,⁽¹⁶⁾ R. Frey,⁽²⁰⁾ K. Furuno,⁽²⁰⁾
 T. Gillman,⁽²⁵⁾ G. Gladding,⁽¹⁴⁾ S. Gonzalez,⁽¹⁶⁾ G.D. Hallewell,⁽²⁷⁾ E.L. Hart,⁽²⁸⁾
 Y. Hasegawa,⁽²⁹⁾ S. Hedges,⁽⁴⁾ S.S. Hertzbach,⁽¹⁷⁾ M.D. Hildreth,⁽²⁷⁾ J. Huber,⁽²⁰⁾
 M.E. Huffer,⁽²⁷⁾ E.W. Hughes,⁽²⁷⁾ H. Hwang,⁽²⁰⁾ Y. Iwasaki,⁽²⁹⁾ D.J. Jackson,⁽²⁵⁾
 P. Jacques,⁽²⁴⁾ J. Jaros,⁽²⁷⁾ A.S. Johnson,⁽³⁾ J.R. Johnson,⁽³²⁾ R.A. Johnson,⁽⁸⁾
 T. Junk,⁽²⁷⁾ R. Kajikawa,⁽¹⁹⁾ M. Kalelkar,⁽²⁴⁾ H. J. Kang,⁽²⁶⁾ I. Karliner,⁽¹⁴⁾
 H. Kawahara,⁽²⁷⁾ H.W. Kendall,⁽¹⁶⁾ Y. Kim,⁽²⁶⁾ M.E. King,⁽²⁷⁾ R. King,⁽²⁷⁾
 R.R. Kofler,⁽¹⁷⁾ N.M. Krishna,⁽¹⁰⁾ R.S. Kroeger,⁽¹⁸⁾ J.F. Labs,⁽²⁷⁾ M. Langston,⁽²⁰⁾
 A. Lath,⁽¹⁶⁾ J.A. Lauber,⁽¹⁰⁾ D.W.G. Leith,⁽²⁷⁾ M.X. Liu,⁽³³⁾ X. Liu,⁽⁷⁾ M. Loreti,⁽²¹⁾
 A. Lu,⁽⁶⁾ H.L. Lynch,⁽²⁷⁾ J. Ma,⁽³¹⁾ G. Mancinelli,⁽²²⁾ S. Manly,⁽³³⁾ G. Mantovani,⁽²²⁾
 T.W. Markiewicz,⁽²⁷⁾ T. Maruyama,⁽²⁷⁾ R. Massetti,⁽²²⁾ H. Masuda,⁽²⁷⁾
 T.S. Mattison,⁽²⁷⁾ E. Mazzucato,⁽¹²⁾ A.K. McKemey,⁽⁴⁾ B.T. Meadows,⁽⁸⁾
 R. Messner,⁽²⁷⁾ P.M. Mockett,⁽³¹⁾ K.C. Moffeit,⁽²⁷⁾ B. Mours,⁽²⁷⁾ G. Müller,⁽²⁷⁾
 D. Muller,⁽²⁷⁾ T. Nagamine,⁽²⁷⁾ U. Nauenberg,⁽¹⁰⁾ H. Neal,⁽²⁷⁾ M. Nussbaum,⁽⁸⁾
 Y. Ohnishi,⁽¹⁹⁾ L.S. Osborne,⁽¹⁶⁾ R.S. Panvini,⁽³⁰⁾ H. Park,⁽²⁰⁾ T.J. Pavel,⁽²⁷⁾
 I. Peruzzi,^{(13)(b)} M. Piccolo,⁽¹³⁾ L. Piemontese,⁽¹²⁾ E. Pieroni,⁽²³⁾ K.T. Pitts,⁽²⁰⁾
 R.J. Plano,⁽²⁴⁾ R. Prepost,⁽³²⁾ C.Y. Prescott,⁽²⁷⁾ G.D. Punkar,⁽²⁷⁾ J. Quigley,⁽¹⁶⁾
 B.N. Ratcliff,⁽²⁷⁾ T.W. Reeves,⁽³⁰⁾ J. Reidy,⁽¹⁸⁾ P.E. Rensing,⁽²⁷⁾ L.S. Rochester,⁽²⁷⁾
 J.E. Rothberg,⁽³¹⁾ P.C. Rowson,⁽¹¹⁾ J.J. Russell,⁽²⁷⁾ O.H. Saxton,⁽²⁷⁾
 S.F. Schaffner,⁽²⁷⁾ T. Schalk,⁽⁷⁾ R.H. Schindler,⁽²⁷⁾ U. Schneekloth,⁽¹⁶⁾
 B.A. Schumm,⁽¹⁵⁾ A. Seiden,⁽⁷⁾ S. Sen,⁽³³⁾ V.V. Serbo,⁽³²⁾ M.H. Shaevitz,⁽¹¹⁾
 J.T. Shank,⁽³⁾ G. Shapiro,⁽¹⁵⁾ S.L. Shapiro,⁽²⁷⁾ D.J. Sherden,⁽²⁷⁾ K.D. Shmakov,⁽²⁸⁾
 C. Simopoulos,⁽²⁷⁾ N.B. Sinev,⁽²⁰⁾ S.R. Smith,⁽²⁷⁾ J.A. Snyder,⁽³³⁾ P. Stamer,⁽²⁴⁾
 H. Steiner,⁽¹⁵⁾ R. Steiner,⁽¹⁾ M.G. Strauss,⁽¹⁷⁾ D. Su,⁽²⁷⁾ F. Suekane,⁽²⁹⁾
 A. Sugiyama,⁽¹⁹⁾ S. Suzuki,⁽¹⁹⁾ M. Swartz,⁽²⁷⁾ A. Szumilo,⁽³¹⁾ T. Takahashi,⁽²⁷⁾

F.E. Taylor,⁽¹⁶⁾ E. Torrence,⁽¹⁶⁾ J.D. Turk,⁽³³⁾ T. Usher,⁽²⁷⁾ J. Va'vra,⁽²⁷⁾
 C. Vannini,⁽²³⁾ E. Vella,⁽²⁷⁾ J.P. Venuti,⁽³⁰⁾ R. Verdier,⁽¹⁶⁾ P.G. Verdini,⁽²³⁾
 S.R. Wagner,⁽²⁷⁾ A.P. Waite,⁽²⁷⁾ S.J. Watts,⁽⁴⁾ A.W. Weidemann,⁽²⁸⁾ E.R. Weiss,⁽³¹⁾
 J.S. Whitaker,⁽³⁾ S.L. White,⁽²⁸⁾ F.J. Wickens,⁽²⁵⁾ D.A. Williams,⁽⁷⁾
 D.C. Williams,⁽¹⁶⁾ S.H. Williams,⁽²⁷⁾ S. Willocq,⁽³³⁾ R.J. Wilson,⁽⁹⁾
 W.J. Wisniewski,⁽⁵⁾ M. Woods,⁽²⁷⁾ G.B. Word,⁽²⁴⁾ J. Wyss,⁽²¹⁾ R.K. Yamamoto,⁽¹⁶⁾
 J.M. Yamartino,⁽¹⁶⁾ X. Yang,⁽²⁰⁾ S.J. Yellin,⁽⁶⁾ C.C. Young,⁽²⁷⁾ H. Yuta,⁽²⁹⁾
 G. Zapalac,⁽³²⁾ R.W. Zdarko,⁽²⁷⁾ C. Zeitlin,⁽²⁰⁾ Z. Zhang,⁽¹⁶⁾ and J. Zhou,⁽²⁰⁾

⁽¹⁾ *Adelphi University, Garden City, New York 11530*

⁽²⁾ *INFN Sezione di Bologna, I-40126 Bologna, Italy*

⁽³⁾ *Boston University, Boston, Massachusetts 02215*

⁽⁴⁾ *Brunel University, Uxbridge, Middlesex UB8 3PH, United Kingdom*

⁽⁵⁾ *California Institute of Technology, Pasadena, California 91125*

⁽⁶⁾ *University of California at Santa Barbara, Santa Barbara, California 93106*

⁽⁷⁾ *University of California at Santa Cruz, Santa Cruz, California 95064*

⁽⁸⁾ *University of Cincinnati, Cincinnati, Ohio 45221*

⁽⁹⁾ *Colorado State University, Fort Collins, Colorado 80523*

⁽¹⁰⁾ *University of Colorado, Boulder, Colorado 80309*

⁽¹¹⁾ *Columbia University, New York, New York 10027*

⁽¹²⁾ *INFN Sezione di Ferrara and Università di Ferrara, I-44100 Ferrara, Italy*

⁽¹³⁾ *INFN Lab. Nazionali di Frascati, I-00044 Frascati, Italy*

⁽¹⁴⁾ *University of Illinois, Urbana, Illinois 61801*

⁽¹⁵⁾ *Lawrence Berkeley Laboratory, University of California, Berkeley, California
 94720*

⁽¹⁶⁾ *Massachusetts Institute of Technology, Cambridge, Massachusetts 02139*

⁽¹⁷⁾ *University of Massachusetts, Amherst, Massachusetts 01003*

- (18) *University of Mississippi, University, Mississippi 38677*
- (19) *Nagoya University, Chikusa-ku, Nagoya 464 Japan*
- (20) *University of Oregon, Eugene, Oregon 97403*
- (21) *INFN Sezione di Padova and Università di Padova, I-35100 Padova, Italy*
- (22) *INFN Sezione di Perugia and Università di Perugia, I-06100 Perugia, Italy*
- (23) *INFN Sezione di Pisa and Università di Pisa, I-56100 Pisa, Italy*
- (24) *Rutgers University, Piscataway, New Jersey 08855*
- (25) *Rutherford Appleton Laboratory, Chilton, Didcot, Oxon OX11 0QX United Kingdom*
- (26) *Sogang University, Seoul, Korea*
- (27) *Stanford Linear Accelerator Center, Stanford University, Stanford, California 94309*
- (28) *University of Tennessee, Knoxville, Tennessee 37996*
- (29) *Tohoku University, Sendai 980 Japan*
- (30) *Vanderbilt University, Nashville, Tennessee 37295*
- (31) *University of Washington, Seattle, Washington 98195*
- (32) *University of Wisconsin, Madison, Wisconsin 53706*
- (33) *Yale University, New Haven, Connecticut 06511*
- † *Deceased*
- (a) *Also at the Università di Genova*
- (b) *Also at the Università di Perugia*

Figure captions

Figure 1.

Normalized distributions of (a) charged particle rapidity for data and Monte Carlo samples. Normalized distributions of (b) event average rapidity gap and (c) event maximum rapidity gap for data, hadronic Monte Carlo and $\tau^+\tau^-$ Monte Carlo samples.

Figure 2.

Normalized distributions of (a) particle rapidity, (b) event average rapidity gap, and (c) event maximum rapidity gap for event generator level with all final state particles, event generator level with charged final state particles, and detector simulation with selection cuts samples.

Figure 3.

Normalized distributions of charged particle rapidity for 2-jet and ≥ 3 -jet events selected by y_{cut} values of (a) 0.005, (b) 0.02, and (c) 0.13. For each jet topology, data and Monte Carlo samples are plotted.

Figure 4.

Normalized distributions of event average rapidity gap for 2-jet and ≥ 3 -jet events selected by y_{cut} values of (a) 0.005, (b) 0.02, and (c) 0.13. For each jet topology, data and Monte Carlo samples are plotted.

Figure 5.

Normalized distributions of event maximum rapidity gap for 2-jet and ≥ 3 -jet events selected by y_{cut} values of (a) 0.005, (b) 0.02, and (c) 0.13. For each jet topology, data and Monte Carlo samples are plotted.

Figure 6.

Normalized distributions of (a) charged particle rapidity, (b) event average rapidity gap, and (c) event maximum rapidity gap for light (u, d and s) and heavy (b) quark samples. For both flavor groups, data and Monte Carlo samples are plotted.

SLD PRELIMINARY

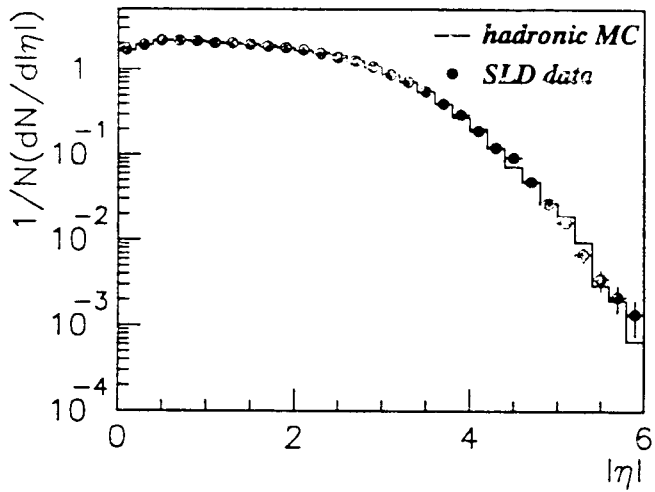


Fig 1a

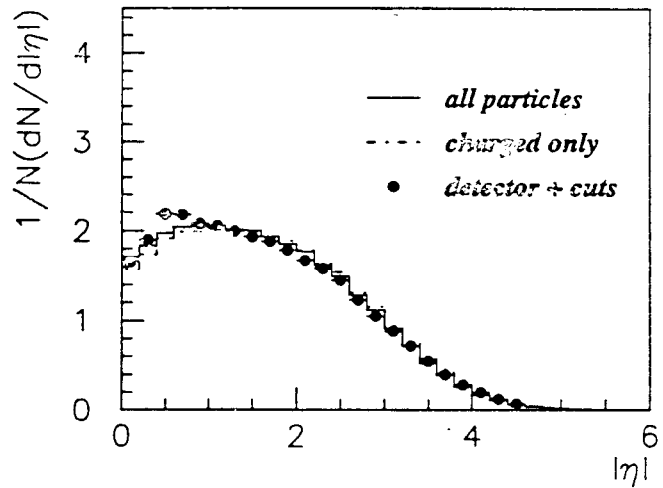


Fig 2a

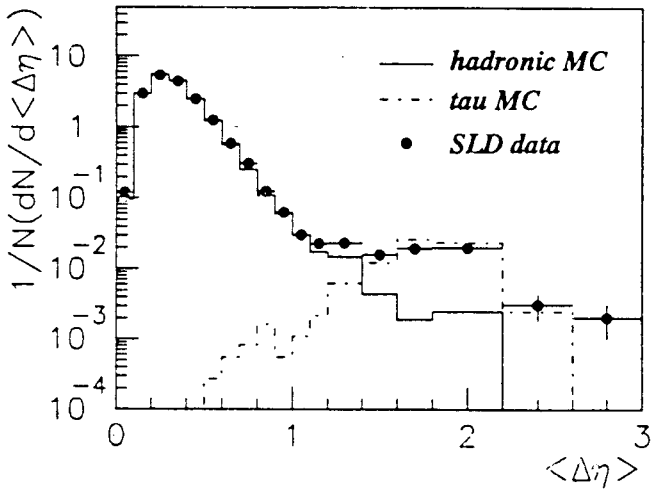


Fig 1b

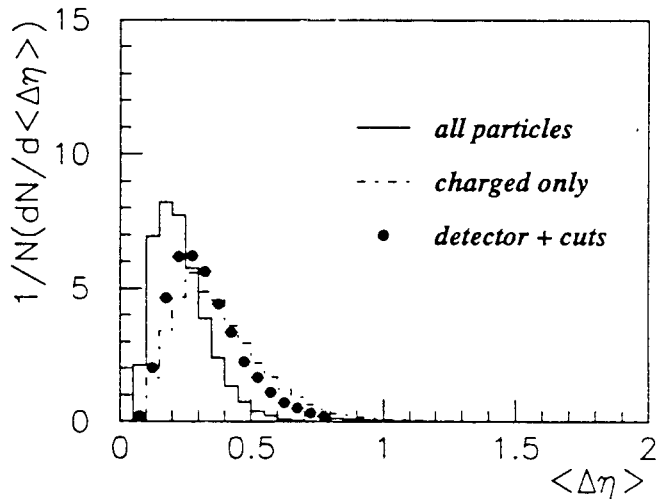


Fig 2b

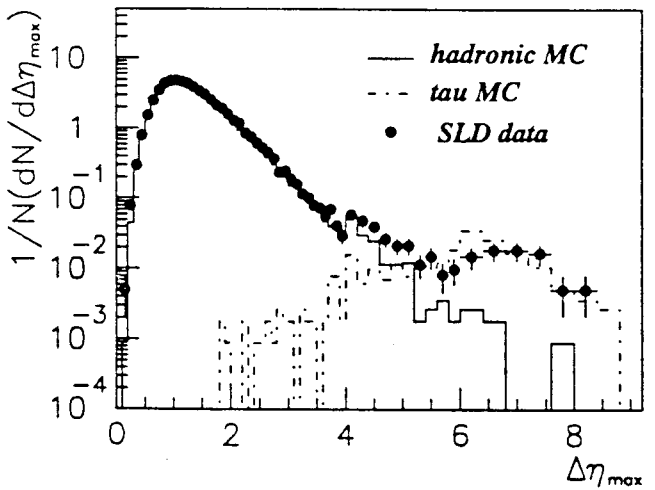


Fig 1c

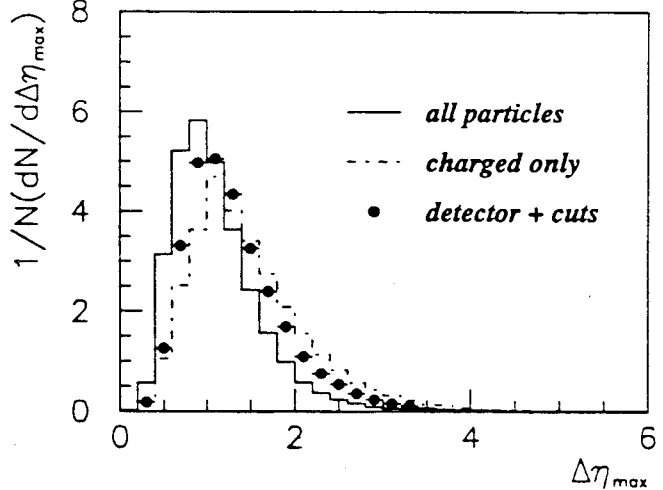


Fig 2c

SLD PRELIMINARY

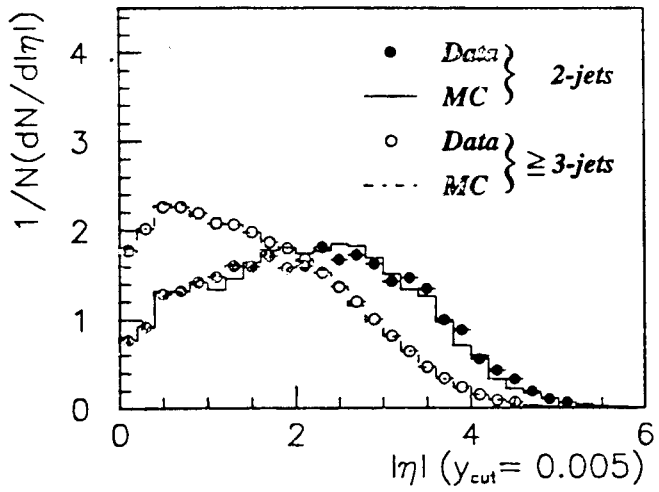


Fig 3a

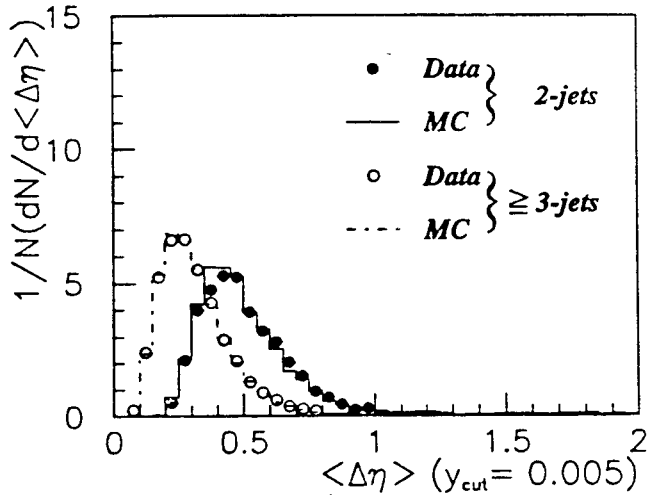


Fig 4a

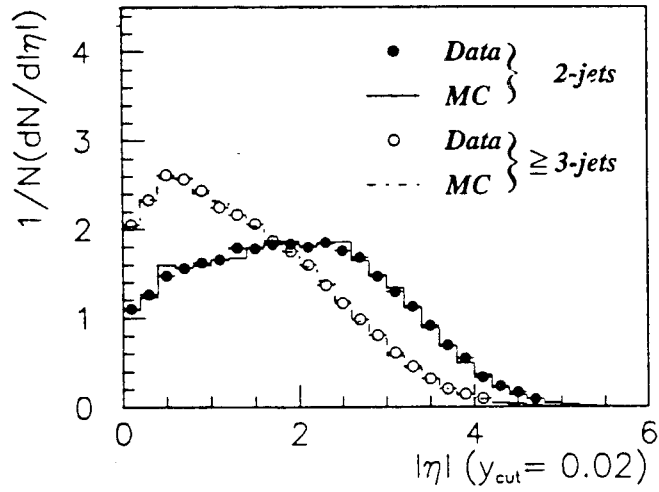


Fig 3b

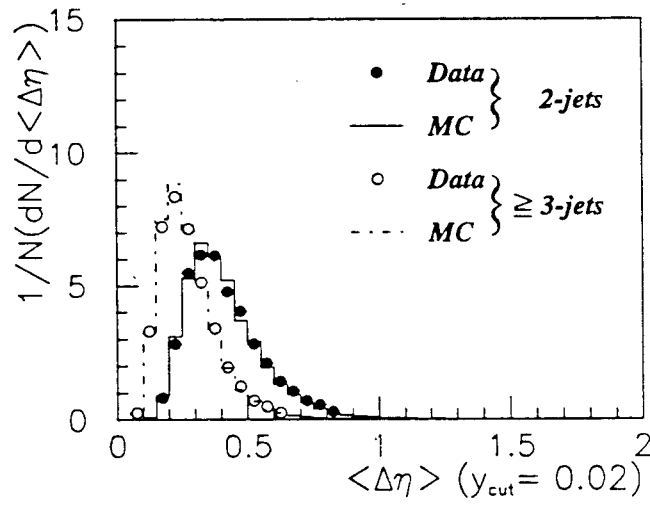


Fig 4b

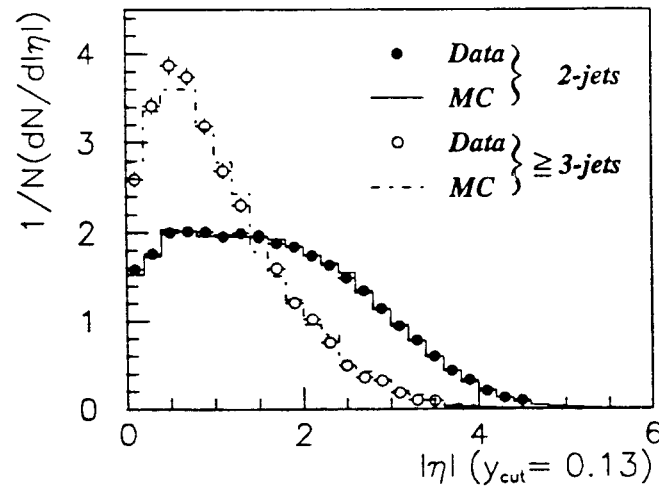


Fig 3c

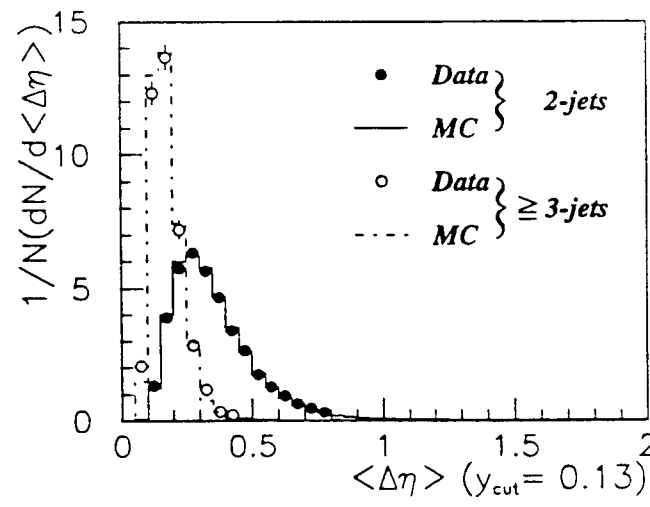


Fig 4c

SLD PRELIMINARY

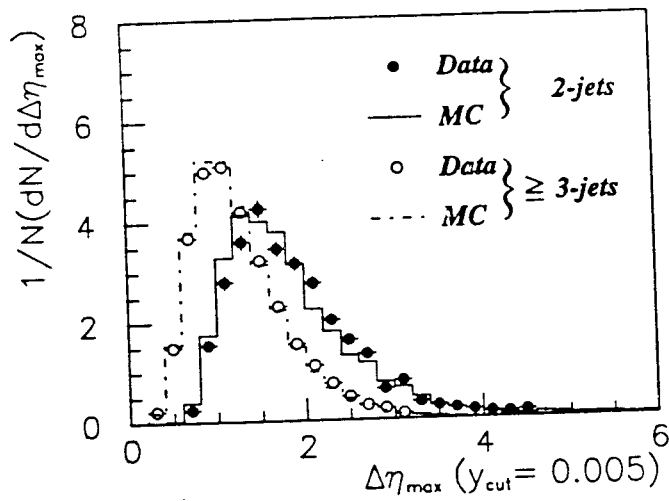


Fig 5a

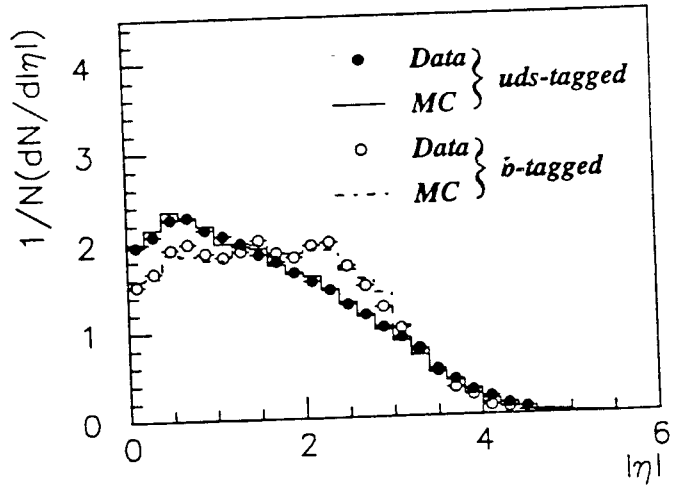


Fig 6a

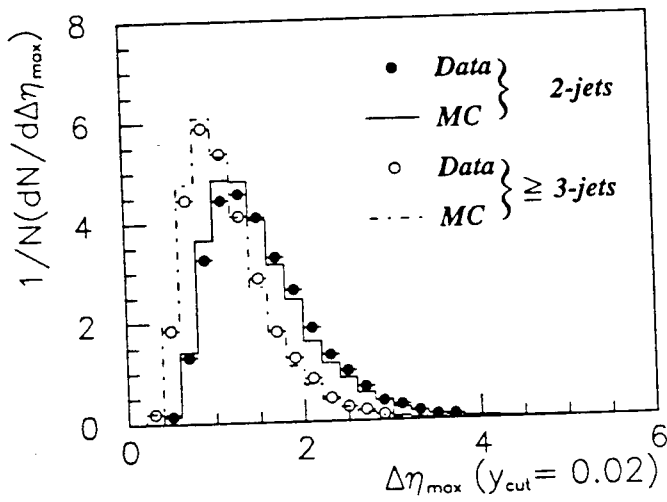


Fig 5b

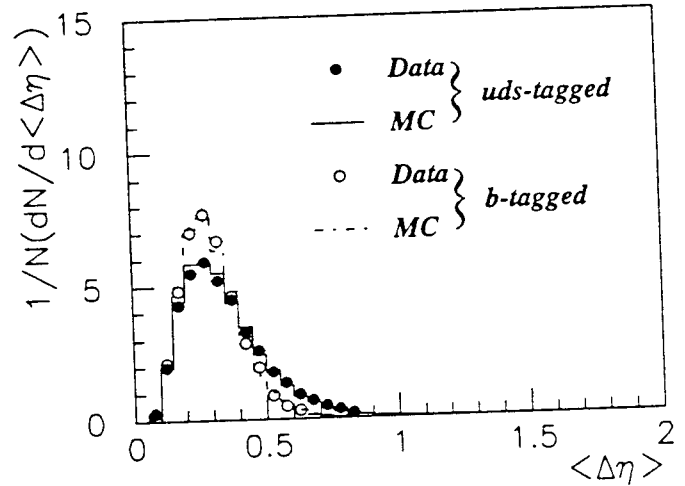


Fig 6b

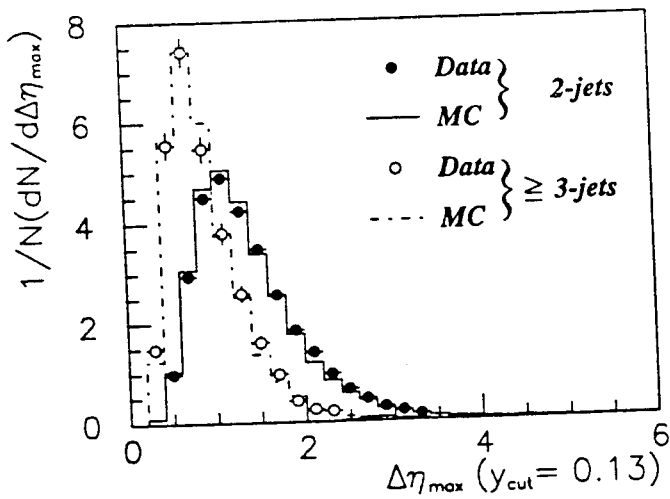


Fig 5c

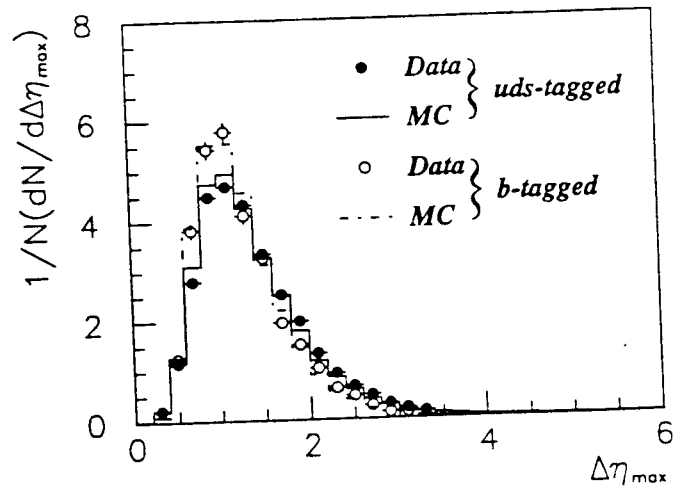


Fig 6c